J Mol Model (2001) 7:398–407
DOI 10.1007/s00894-001-0057-6

ORIGINAL PAPER

Cenk Selçuki · Viktorya Aviyente

An ab initio study of the formation of alkoxy radicals by reactions of simple alkenes with the OH radical

Received: 12 July 2001 / Accepted: 8 October 2001 / Published online: 15 November 2001

Abstract The formation of ethoxy, propoxy and butoxy radicals in the reactions of ethene, propene, *cis*- and *trans*-2-butene with the OH radical has been modeled in the gaseous phase at the MP2/6-31+G(d) level. All the possible reaction pathways have been investigated, and the structures as well as the energetics have been determined. The reactants, prereaction complexes, transition states and products located along the alkene–OH radical reaction coordinates have been discussed thoroughly. The rate determining step for these reactions is the conversion of hydroxyalkyl radicals to alkoxy radicals. The reaction barriers and exothermicities for these small alkenes are more or less identical for the compounds studied. Nevertheless, addition of OH to the central carbon atom of propene is slightly favored kinetically and thermodynamically (1 kcal mol^{-1}) over the others.

Keywords Alkene · Hydroxyl radical · Prereaction complex · Alkoxy radical

Introduction

Reactions of ozone with alkenes have great importance for both gas- and liquid-phase chemistry. [1, 2] These reactions constitute one of the most important classes of atmospheric chemical reactions. [2]

The formation and reactions of the OH radical in the ozonolysis of alkenes have been studied by several groups. [3, 4, 5, 6, 7, 8, 9, 10, 11, 12, 13, 14, 15, 16] Atkinson and Aschmann have studied the OH production from the gas phase reactions of ozone with a series of alkenes including propene, *cis*- and *trans*-2-butene under atmospheric conditions, where they have used cyclohexane as the scavenger. [3] Grosjean et al. have identified and measured the carbonyl and carboxylic acid products of the ozone–olefin reactions where OH is produced. [4] Paulson and Orlando have determined HO_x yields for alkene–ozone reactions for different alkenes and their results have shown that ozonolysis reactions are important sources of HO_x radicals. [5] Paulson et al. have investigated the OH yields for the reactions of terminal alkenes including propene and have explained the relation between the structure of the alkene and OH formation. [6] Most recently, the formation of OH radicals in gas phase reactions of propene, isobutene and isoprene with ozone has been investigated by Neeb and Moortgat. [7] Their results have shown that OH forms mostly via a unimolecular process, presumably during the decomposition of carbonyl oxide intermediates.

The reactions of OH with alkenes have been studied both experimentally and computationally since these reactions are very important for atmospheric chemistry. Martinez et al. have studied the reactions of OH with *trans*-2-butene and have investigated the reactions of hydroxy substituted alkyl radicals formed as secondary products during ozonolysis. [8] The intermediates have been determined by using photoionization mass spectroscopy and the product has been found to be 2-hydroxy-1-methylpropyl radical. Tully used laser-based chemical kinetics techniques to investigate the ethene–OH reaction. [9] In their detailed study, Zellner and Lorenz have measured the rate constants for the ethene–OH and propene–OH reactions by taking into account the activated complex forms. [10] Atkinson has determined the rate constants for OH addition to carbon–carbon double and triple bonds. [11] Approximately 300 compounds have been studied and structure–activity relationships for the estimation of the rate constants for these compounds in the gas phase have been investigated. Wei-Guang Diau and Lee [12] have measured the rate coefficients and enthalpy change of the equilibrium reaction between ethene–OH and C_2H_4OH radical. Hatakeyama et al. have studied the formation of 2-hydroxyethyl hydroperoxide in an OH initiated reaction of ethene in air in the absence of NO. [13]

Sosa and Schlegel have modeled the reactions of OH with ethene and acetylene. [14] The values obtained by

C. Selçuki · V. Aviyente (✉)
Chemistry Department, Boğaziçi University, 80815, Bebek, Istanbul, Turkey
e-mail: aviye@hamlin.cc.boun.edu.tr
Tel.: +90-212-2631540 x 1610, Fax: +90-212-2872467

annihilation of the largest spin contaminant combined with electron correlation were found to be in good agreement with the experimental activation energies. In their further study, [15] Sosa and Schlegel have studied the energetically favorable reaction path for the unimolecular decomposition of the primary addition product of the ethene–OH reaction. They found that the most favorable path is the formation of 2-hydroxyethyl radical, which then rearranges to ethoxy radical, followed by the decomposition process, which yields methyl radical and formaldehyde. Abbatt and Anderson have determined the rate constants for the reactions of halosubstituted ethenes with OH radical. [16] They also explained the kinetics and mechanism of these reactions by frontier orbital analysis, in which they modeled the ethene–OH reaction at the UHF/6-31G** level. Villà et al. have investigated the activation energy trends for the formation of C_2H_4OH as a result of OH addition to ethene. [17] Their results reveal a monotonic increase in energy without a recombination barrier, similar to the MRD-CI results of Engels and coworkers obtained for Cl- and F-substituted ethenes. [18, 19] Recently, Alvarez-Idaboy et al. have studied the propene–OH reaction in detail and obtained the complete energy surface of the reaction mechanism in the gas phase as a model for an inert atmosphere. [20] Reactions of ethene and its mono chloro- and fluoro-substituted analogs with OH have been investigated by Sekusak et al. [21] Yamada et al. have studied the kinetic and thermodynamic properties of OH addition to ethene by taking into account the adduct formation, isomerization and isomer dissociation reactions with the G2 and CBS methods. [22] In a very recent study, Alvarez-Idaboy et al. have explained the negative activation energies in OH addition to substituted ethenes by means of classical transition state theory and quantum chemical calculations. [23]

In this paper, we have investigated the formation of alkoxy radicals as a result of the reactions of OH radical with four alkenes; ethene, propene, *cis*- and *trans*-2-butene. There have been numerous computational studies reported for the reactions of the first two alkenes with OH radical, [8, 9, 10, 11, 12, 13, 14, 15, 16, 17, 20, 21, 22, 23] but to the best of our knowledge, this will be the first computational study on the reactions of the other two alkenes with OH radical.

Methodology

All the geometries have been located with the second order Møller–Plesset (MP2) approach [24, 25] with the frozen core approximation for the formation of alkoxy radicals in alkene–OH radical reactions. The 6-31+G(d) basis set, which is augmented with polarization and diffuse functions on heavy atoms, has been used.

The nature of the structures (minimum or transition state) has been verified using the Hessian matrix eigenvalues.

Both MP2 and spin projected MP2 (PMP2) energies have been discussed for the reaction paths since it has been shown that PMP2 values yield energy differences that are in far better agreement with experimental values. [20]

Calculations have been carried out with Gaussian 94 (Revision C.3). [26]

Results and discussion

The schematic reaction path for formation of alkoxy radicals in the alkene–OH reactions is given in Fig. 1. The structures are numbered from **1** to **6** except for the OH radical. The initials of each alkene precede the number of the corresponding structure in the following discussion (i.e. **e2** stands for the prereaction complex for ethene). For the reaction of propene, two different path-

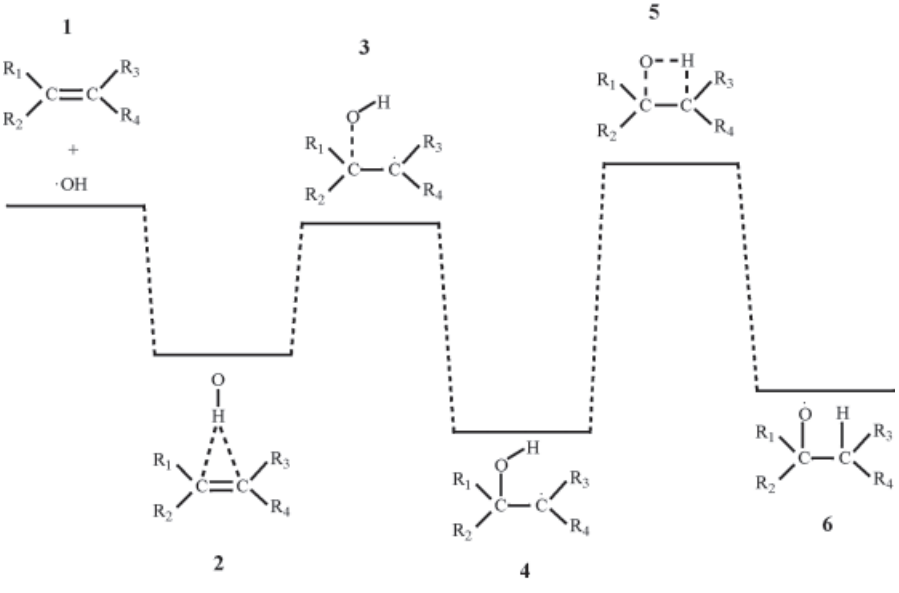

Fig. 1 Schematic representation of the formation of alkoxy radicals in the alkene–OH reaction

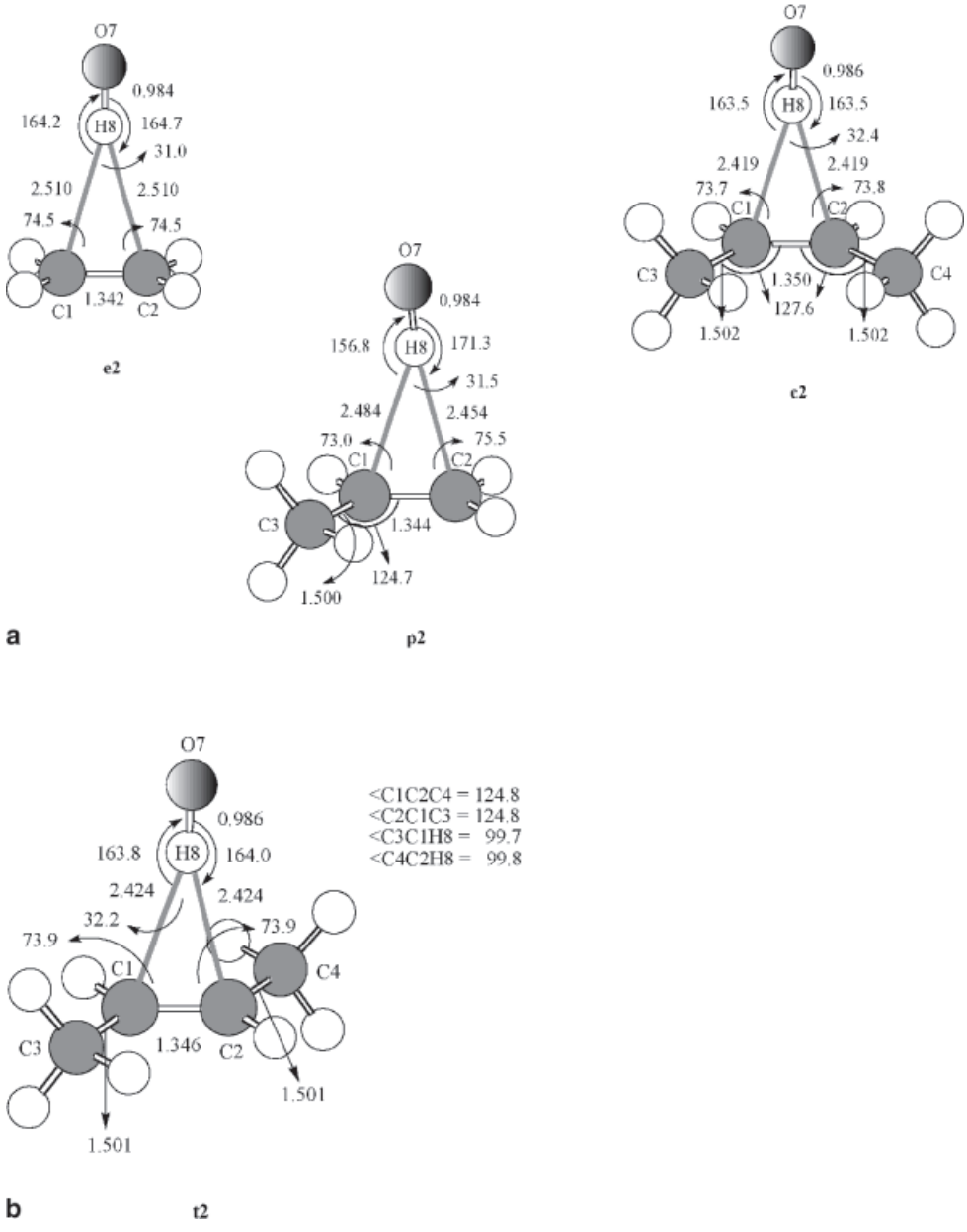

Fig. 2 **a** The optimized structures of the alkene–OH complexes for ethene (**e2**), propene (**p2**) and *cis*-2-butene (**c2**); bond lengths in Å, bond angles and dihedral angles are in degrees. **b** The optimized structures of the alkene–OH complexes for *trans*-2-butene (**t2**); bond lengths in Å, bond angles and dihedral angles are in degrees

ways are present; the structures corresponding to the OH addition to the central carbon atom are represented by **p** and those corresponding to the OH addition to the terminal carbon atom are shown with **p′**. The optimized structures for the alkene–OH complexes, transition states for OH addition to the alkenes and transition states for hydrogen transfer are given in Figs. 2, 3, 4, 5 and 6. Table 1 gathers the total electronic energies (E_{TOT}) and zero-point energies (ZPE) of the OH radical and the alkenes studied. The ZPE values are used without any scaling. The average values of the square of the spin angular momentum, $\langle S^2 \rangle$, for all the compounds before and after the projection are given in Table 2. The relative energies of the compounds studied are given in Table 3 (MP2 and PMP2) in order to emphasize the effect of projection on the energetics of the studied compounds. The numbering system of the atoms within each structure is similar for all compounds.

The following discussion on the energetics of the alkene–OH reactions is based on the PMP2 values (without ZPE corrections) unless otherwise stated.

Ethene–OH reaction

The addition of the OH radical to ethene (**e1**) occurs via the formation of the prereaction complex (**e2**). As has been indicated earlier, most of the radical additions to the unsaturated carbon–carbon double bonds have negative activation barriers as explained by the formation of prereaction complexes lower in energy than the separated reactants. [27, 28] Complex **e2** is formed by the weak

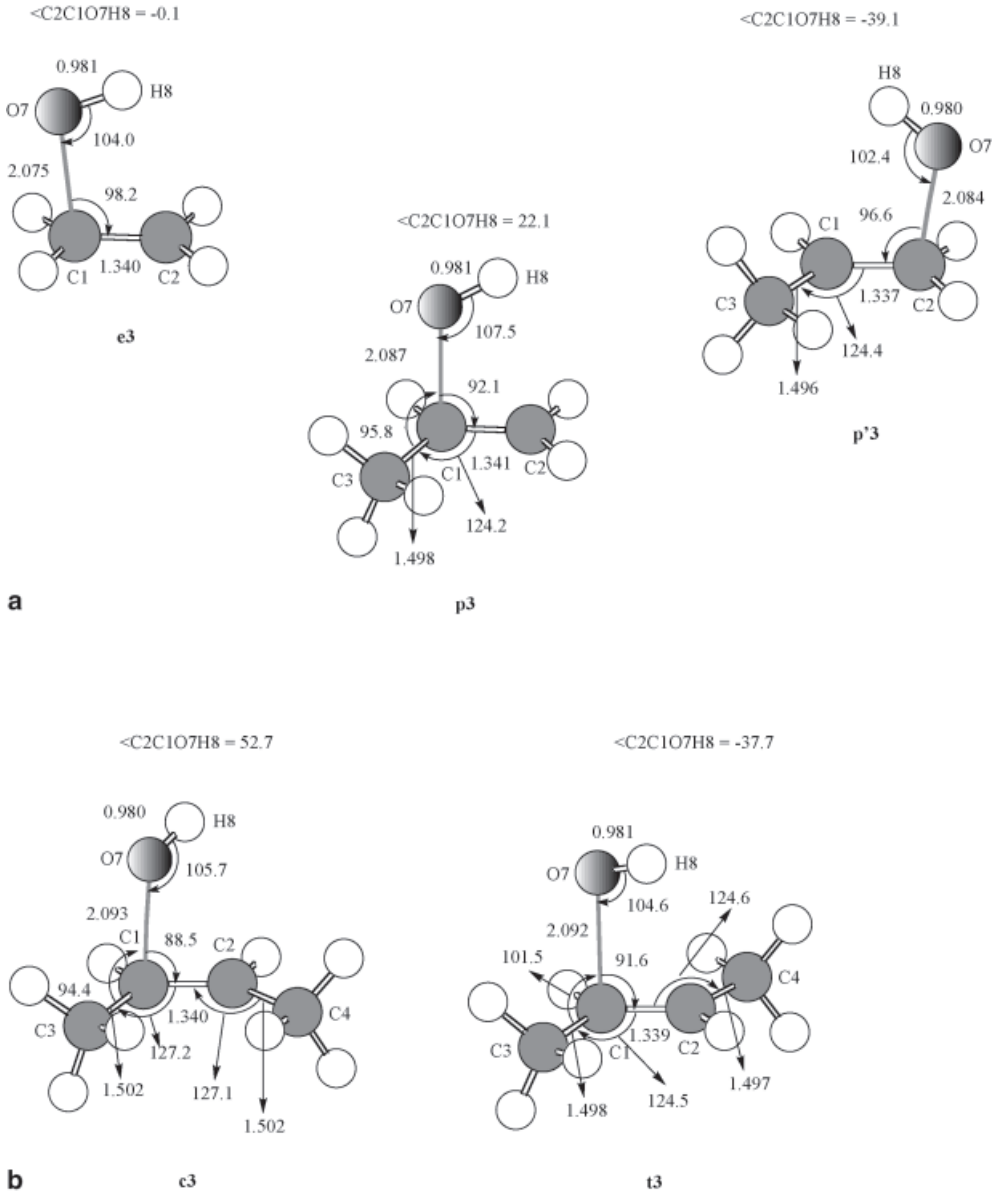

Fig. 3 **a** The optimized structures of the transition states for the OH addition to ethene (**e3**), propene (**p3**, **p′3**); bond lengths in Å, bond angles and dihedral angles are in degrees. **b** The optimized structures of the transition states for the OH addition to *cis*-2-butene (**c3**) and *trans*-2-butene (**t3**); bond lengths in Å, bond angles and dihedral angles are in degrees

Table 1 Total electronic energies (E_{TOT}; in Hartrees) and zero-point vibrational energies (ZPE; in Hartrees) of the OH radical and studied alkenes calculated at the MP2/6-31+G(d) level

	E_{TOT}	ZPE
OH[a]	–75.5296357	0.008458
Ethylene (**e1**)	–78.2911795	0.051792
Propene (**p1**)	–117.4629407	0.081110
cis-2-Butene (**c1**)	–156.6317980	0.110047
trans-2-Butene (**t1**)	–156.6342252	0.110015

[a] PMP2 energy is –75.5313329 Hartrees

interactions between the hydrogen of the OH radical and the electron-rich double bond of ethene (Fig. 2a). Complex **e2** is almost symmetric, having identical values for the C1H8 and C2H8 bonds as well as for the C1C2H8 and C2C1H8 angles. A difference of 0.5° between the C1H8O7 and C2H8O7 angles changes the point group from C_{2v} to C_s. The C1C2 bond length is slightly longer than the corresponding bond in ethene (**e1**) (1.340 Å).

The transition state **e3** seems to be a loose (or an early) transition state due to the long C1O7 bond (2.075 Å). The OH is almost planar with the carbon–carbon double bond with a very small deviation of 0.1° from the C2C1O7 plane (Fig. 3a).

Two conformers were optimized for the hydroxyethyl radical (**e4**). Both have almost similar geometrical parameters except for the position of the hydroxyl hydrogen (Fig. 4a), which is directed either inwards or outwards. Only the more stable conformer where hydrogen is directed inwards is considered in this study. The inwards orientation of the hydroxyl hydrogen increases the C2C1O7 angle by ~4.5°.

The next transition state (**e5**) shows the migration of the hydroxyl hydrogen to C2 to form the ethoxy radical

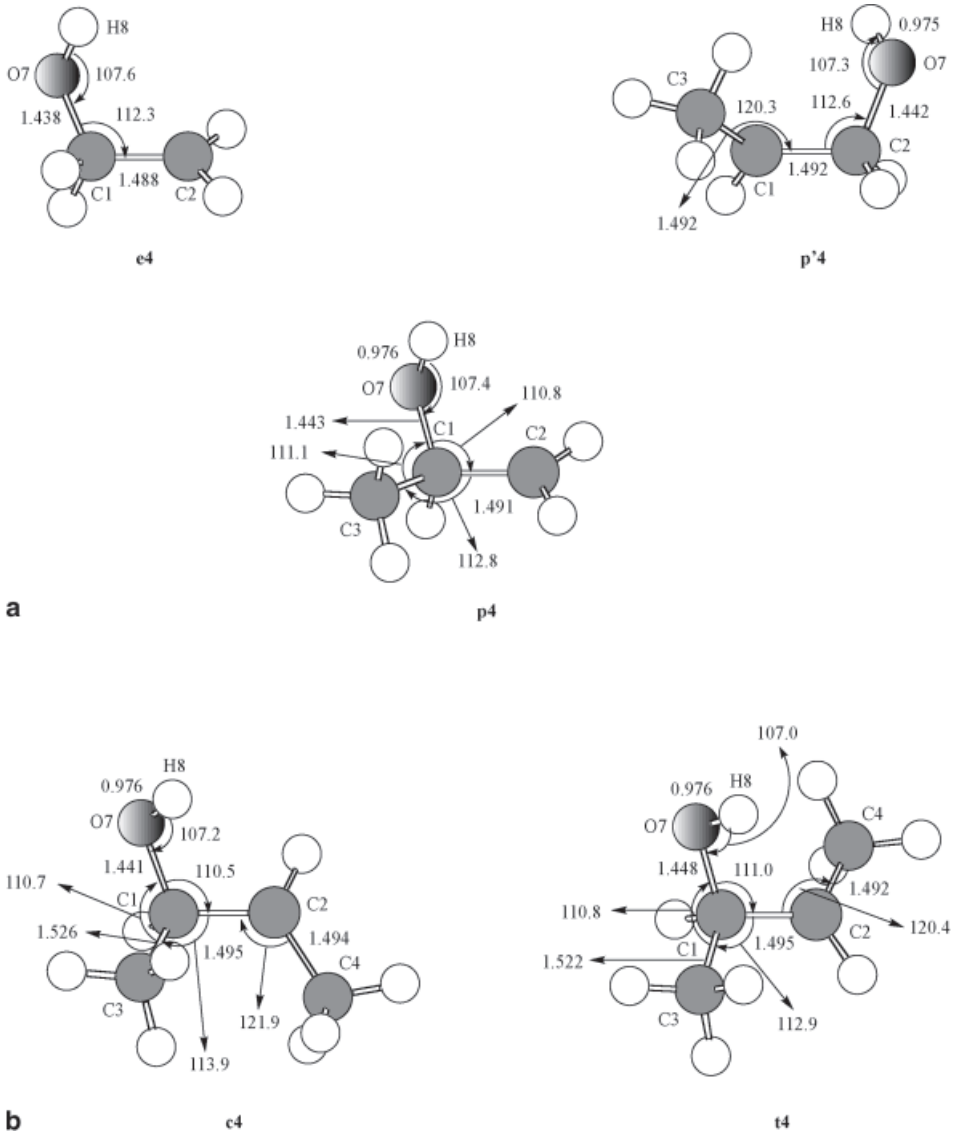

Fig. 4 **a** The optimized structures of hydroxyethyl (**e4**), hydroxypropyl (**p4**, **p′4**) radicals; bond lengths in Å, bond angles and dihedral angles are in degrees. **b** The optimized structures of hydroxybutyl (*cis*-2-butene, **c4**); (*trans*-2-butene, **t4**) radicals; bond lengths in Å, bond angles and dihedral angles are in degrees

Table 2 $\langle S^2 \rangle$values before ($\langle S^2_i \rangle$) and after ($\langle S^2_f \rangle$) the projection for the structures optimized for the OH+alkene reactions at the MP2/6-31+G(d) level

	Ethylene			Propene			*cis*-2-Butene			*trans*-2-Butene	
	$\langle S^2_i \rangle$	$\langle S^2_f \rangle$		$\langle S^2_i \rangle$	$\langle S^2_f \rangle$		$\langle S^2_i \rangle$	$\langle S^2_f \rangle$		$\langle S^2_i \rangle$	$\langle S^2_f \rangle$
OH	0.7565	0.7500	OH	0.7565	0.7500	OH	0.7565	0.7500	OH	0.7565	0.7500
e1	–	–	**p1**	–	–	**c1**	–	–	**t1**	–	–
e2	0.7564	0.7500	**p2**	0.7564	0.7500	**c2**	0.7564	0.7500	**t2**	0.7564	0.7500
e3	0.9482	0.7555	**p3**	0.9269	0.7547	**c3**	0.9088	0.7541	**t3**	0.9184	0.7545
e4	0.7622	0.7501	**p′3**	0.9359	0.7551	**c4**	0.7627	0.7501	**t4**	0.7632	0.7501
e5	0.7970	0.7508	**p4**	0.7622	0.7501	**c5**	0.7962	0.7508	**t5**	0.7965	0.7508
e6	0.7590	0.7501	**p′4**	0.7632	0.7501	**c6**	0.7588	0.7501	**t6**	0.7590	0.7501
			p5	0.7970	0.7508						
			p′5	0.7965	0.7508						
			p6	0.7589	0.7501						
			p′6	0.7590	0.7501						

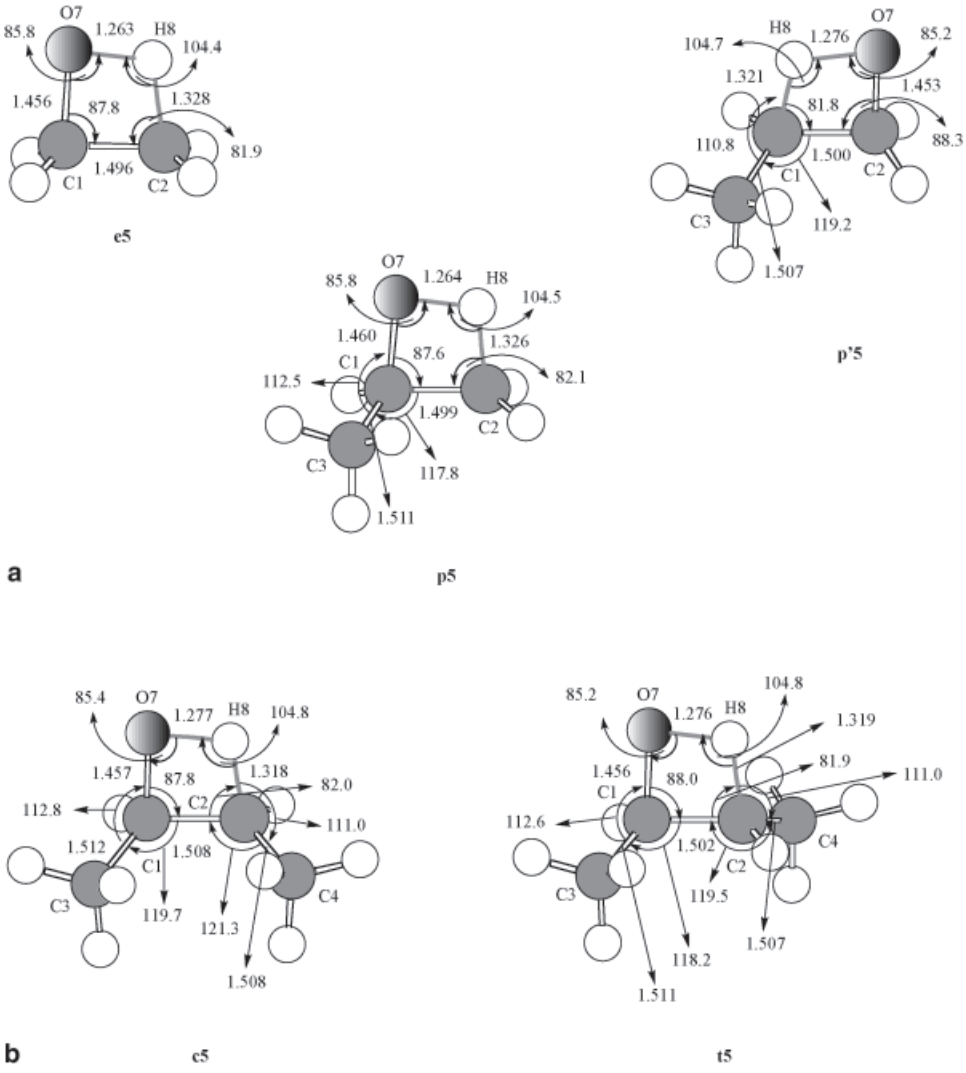

Fig. 5 **a** The optimized structures of the transition states for conversion of hydroxyalkyl radicals to alkoxy radicals; for ethene (**e5**) and propene (**p5**, **p′5**); bond lengths in Å, bond angles and dihedral angles are in degrees. **b** The optimized structures of the transition states for conversion of hydroxyalkyl radicals to alkoxy radicals; for *cis*-2-butene (**c5**) and *trans*-2-butene (**t5**); bond lengths in Å, bond angles and dihedral angles are in degrees

(**e6**). All four atoms (C1, C2, O7 and H8) lie in the same plane and the transition state seems a tight transition state due to the strong C2H8 and O7H8 bonds (Figs. 5a and 6a).

One conformer for the ethoxy radical (**e6**) in which the methyl hydrogens are staggered to the oxygen has been located as a stationary point (Fig. 6a). As expected, the C1C2 bond has the length of a carbon–carbon single bond. Additionally, the C2C1O7 angle (106.0°) is smaller than the tetrahedral angle of 109.5° due to the attractions between the oxygen lone pair and the methyl hydrogens.

The ethene–OH reaction starts with the formation of the complex **e2**. This complex is 3.36 kcal mol^{-1} lower in energy than the initial reactants, OH radical and ethene (**e1**). The transition state **e3**, energetically more stable than the reactants, has a very low barrier of 1.99 kcal mol^{-1} as compared to **e2** (Table 3). This behavior has been observed in most of the alkene–radical reactions as indicated in the literature. [20, 21, 27, 28] As seen in Table 2, the $\langle S^2 \rangle$ value for the transition state **e3** (0.9482) is larger than the expected value for a doublet state (0.7500); but it is well corrected by the projection (0.7555). Similar larger values are obtained for the other corresponding transition states (**p3**, **p′3**, **c3** and **t3**) for the studied alkene–OH reactions (Table 2). The spin contamination for the other optimized structures (intermediates, transition states and alkoxy radicals) is almost negligible. However, it is worth noting that the differences in the MP2 and PMP2 energies increase with the increasing spin contamination as expected (Table 3). The hydroxyethyl radical (**e4**) has a relative energy of –31.96 kcal mol^{-1}, in good agreement with the results of Bartels et al. [29] and earlier computational studies. [15, 16, 17, 20] The transition state **e5** is slightly higher in energy (3.48 kcal mol^{-1}) than the initial reactants, similar to the value calculated by Alvarez-Idaboy et al. at a similar level [20], whereas Bartels et al. [29] suggested a value of $\leq$2 kcal mol^{-1} in qualitatively good agreement with our result. The relative energy calculated for the ethoxy radical **e6** is –28.13 kcal mol^{-1} as compared to the experimental value of –25.9 kcal mol^{-1} proposed by Bartels et al. [29] The results obtained in previous computations also assign values similar to ours. [15, 16, 17,

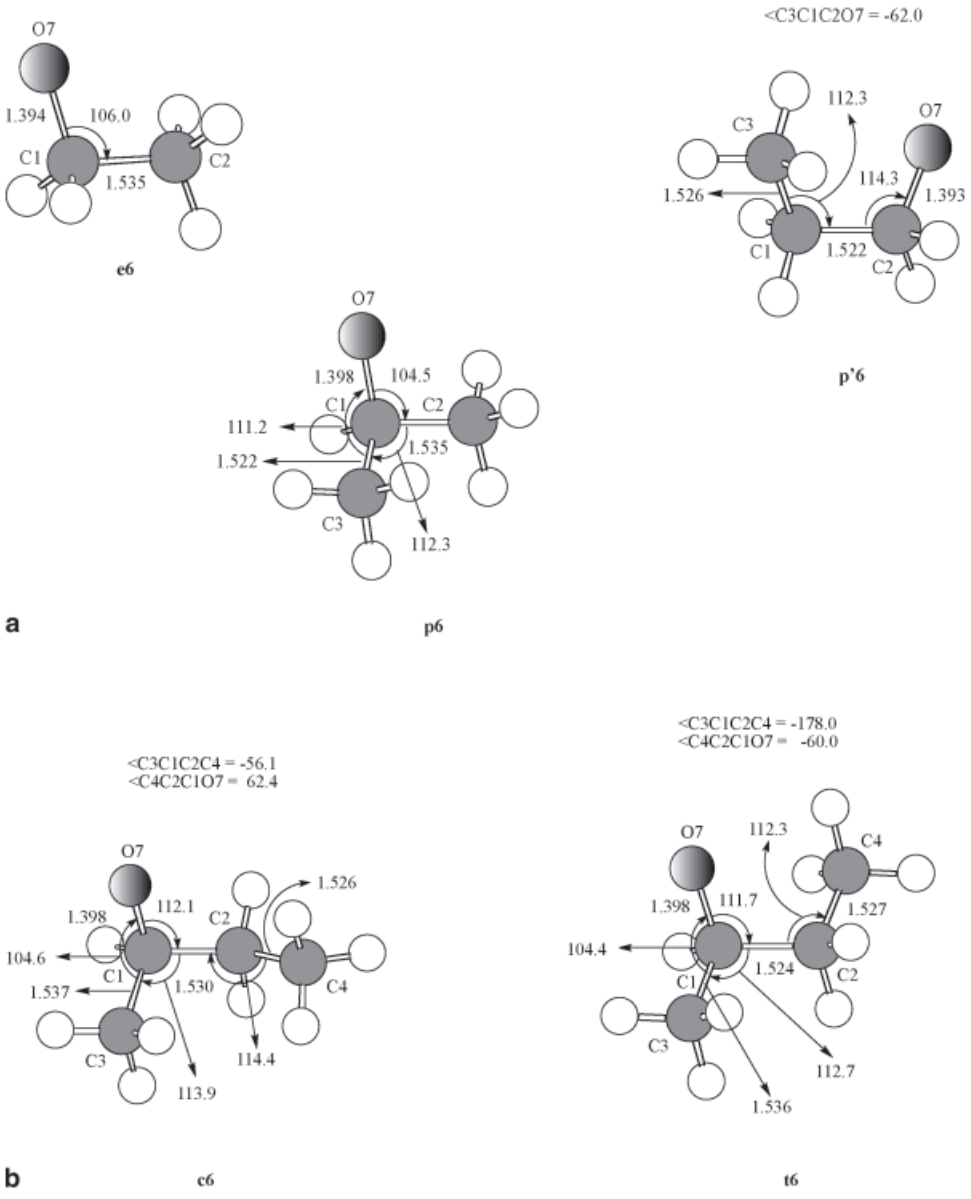

Fig. 6 **a** The optimized structures of ethoxy (**e6**) and propoxy (**p6**, **p′6**) radicals; bond lengths in Å, bond angles and dihedral angles are in degrees. **b** The optimized structures of butoxy (*cis*-2-butene, **c6**) (*trans*-2-butene, **t6**) radicals; bond lengths in Å, bond angles and dihedral angles are in degrees

20, 21, 22] The PMP2 result for the relative energy of the ethoxy radical **e6** is higher by ~2.0–2.5 kcal mol^{-1} as compared to the experimental results but the barriers and the endothermic behavior of the reaction are reproduced quite well with this level of theory.

Propene–OH reaction

The reaction between propene (**p1**) and OH radical has interesting features that are different from the other studied alkenes. Propene is the mono methyl substituted ethene and this causes two nonequivalent carbon atoms to be susceptible to attack by the OH radical: one is the central carbon atom (C1) and the other is the terminal carbon atom (C2). In the literature, there are contradictory results about the most favorable site for the OH attack. [30, 31] Cvetanovic [30] has reported that most of the attack occurs on the terminal carbon, whereas the results of Diaz-Acosta et al. [31] have shown that OH addition occurs mainly on the central carbon.

In the reaction path of the propene (**p1**), the reaction is thought to proceed through the prereaction complex (**p2**) (Fig. 2a). Due to the presence of the electron donating methyl group the CC double bond is now more electron rich as compared to ethene (**e1**) and the attraction between propene and OH radical is stronger, as observed by the shortening of the C1H8 and C2H8 bonds in **p2** (Fig. 2a).

There are two optimized conformers of the transition state (**p3** and **p′3**) for the addition of the OH radical to propene (Fig. 3a). The OH radical adds to the central carbon in **p3**, whereas it adds to the terminal carbon in **p′3**. The geometries (especially bond lengths) for **p3** and **p′3** do not differ very much. However, the differences in bond angles show that the steric factors are effective;

Table 3 Relative MP2 (top) and PMP2 (bottom) energies (kcal mol^{-1}) for the alkene–OH radical reactions calculated for the possible pathways. Values in parentheses include zero-point energies

	ET			PR1			PR2	
OH+**e1**	0.00	(0.00)	OH+**p1**	0.00	(0.00)	OH+**p1**	0.00	(0.00)
e2	–3.38	(–1.45)	**p2**	–4.05	(–2.56)	**p2**	–4.05	(–2.56)
e3	5.50	(8.06)	**p3**	4.21	(6.71)	**p′3**	4.85	(7.42)
e4	–31.77	(–27.80)	**p4**	–32.63	(–29.08)	**p′4**	–31.65	(–27.60)
e5	6.59	(8.83)	**p5**	4.54	(6.30)	**p′5**	7.01	(9.26)
e6	–27.91	(–22.86)	**p6**	–29.33	(–24.48)	**p′6**	–25.89	(–21.87)
	CB		TB					
OH+**c1**	0.00	(0.00)	OH+**t1**	0.00	(0.00)			
c2	–4.69	(–3.21)	**t2**	–4.57	(–3.11)			
c3	3.15	(5.72)	**t3**	3.53	(6.01)			
c4	–33.78	(–29.80)	**t4**	–32.97	(–29.24)			
c5	4.13	(6.13)	**t5**	4.42	(6.38)			
c6	–27.76	(–22.72)	**t6**	–26.90	(–21.86)			
	ET		PR1			PR2		
OH+**e1**	0.00	(0.00)	OH+**p1**	0.00	(0.00)	OH+**p1**	0.00	(0.00)
e2	–3.36	(–1.43)	**p2**	–4.03	(–2.54)	**p2**	–4.03	(–2.54)
e3	–1.99	(0.58)	**p3**	–2.52	(–0.02)	**p′3**	–2.24	(–0.33)
e4	–31.96	(–28.00)	**p4**	–32.82	(–29.27)	**p′4**	–31.92	(–27.86)
e5	3.48	(5.71)	**p5**	1.42	(3.19)	**p′5**	3.94	(6.18)
e6	–28.13	(–23.08)	**p6**	–29.54	(–24.70)	**p′′′′6**	–26.12	(–22.10)
	CB		TB					
OH+**c1**	0.00	(0.00)	OH+**t1**	0.00	(0.00)			
c2	–4.67	(–3.19)	**t2**	–4.55	(–3.10)			
c3	–3.01	(–0.43)	**t3**	–2.95	(–0.47)			
c4	–34.01	(–30.03)	**t4**	–33.25	(–29.52)			
c5	1.08	(3.08)	**t5**	1.34	(3.31)			
c6	–27.97	(–22.93)	**t6**	–27.12	(–22.09)			

i.e., the C1C2O7 angle in **p′3** is larger than the C2C1O7 angle in **p3** by 4.5° since the OH group faces the methyl group in **p′3** whereas it is on the same carbon as the methyl group in **p3**.

There are two conformers for each of the hydroxypropyl radicals (Fig. 4a) **p4** and **p′4**. As in the case of the hydroxyethyl radical the only difference between the conformers is the orientation of the OH hydrogen, and the conformers where this hydrogen is directed inwards are more stable. Due to the repulsive interactions between the OH group and the methyl group, the C1C3 bond lengths are longer in **p4** than in **p′4**.

Two transition states for the hydrogen transfer from the OH group to the central or terminal carbon have been optimized. In **p5** the hydrogen has moved to the terminal carbon, whereas in **p′5** it has moved to the central carbon. The main difference between the geometries of these two transition states lies in the O7H8 bond, which is 0.012 Å shorter in **p5** enabling a hydrogen transfer (Fig. 5a).

Two conformers for the propoxy radical **p′6** have been located, whereas there is only one conformer for **p6** (Fig. 6a). The oxygen is located on the central carbon in **p6**, whereas it is placed on the terminal carbon in the conformers of **p′6**. The geometry of **p6** differs significantly from the conformers of **p′6**. The C1C2 bond is 0.013 Å longer in **p6** as compared to the same bond in the conformers of **p′6**. Furthermore, in **p6** the C1C3 bond is shorter and the CO bond is longer than in **p′6**. These observations can be explained by the electron withdrawing ability of the oxygen atom, which is more effective when it is on the same carbon as the methyl group. As the electron flow is through the atoms C3, C1 and O7, the C1C3 bond shortens whereas the C1C2 and C1O7 bonds lengthen. In the other two conformers of **p′6**, the electron flow occurs through the atoms C3, C1, C2 and O7, producing opposite changes for the bond lengths discussed above. The geometries of the conformers of **p′6** differ only in the position of methyl group with respect to the oxygen atom, the other parameters being similar.

Although there are two different pathways, the reaction starts with the formation of a single propene–OH complex (**p2**), which is 4.03 kcal mol^{-1} lower in energy than the initial reactants, OH radical and **p1** (Table 3). The transition state for the OH addition to the central carbon atom (**p3**) is slightly more stable (0.28 kcal mol^{-1}) than that for the OH addition to the terminal carbon atom (**p′3**). Computations by Alvarez-Idaboy et al. have reproduced this difference as 0.4 kcal mol^{-1}, in agreement with our results. [20] This difference increases to 0.9 kcal mol^{-1} for the corresponding hydroxypropyl radicals **p4** and **p′4**. Alvarez-Idaboy et al. have calculated a more significant difference of 2.7 kcal mol^{-1} for the

hydroxypropyl radical conformers. [20] Regarding the transition states for the hydrogen transfer, **p5** is more stable than **p′5** by 2.52 kcal mol^{-1} (Table 3), which is ~1.1 kcal mol^{-1} lower than the value calculated earlier. [20] It is worth noting that both of the transition states **p5** and **p′5** are higher in energy than the initial reactants, as in the case of ethene (Table 3). Considering the stabilities of the propoxy radicals **p6** and **p′6**, the radical where the oxygen atom is located on the more substituted carbon atom is energetically more stable, i.e. **p6** is 3.42 kcal mol^{-1} more stable than **p′6** but Alvarez-Idaboy et al. assign a difference of 5.2 kcal mol^{-1}, significantly higher than our result. [20] The path where the reaction proceeds through the OH attack on the central carbon atom (path containing structures shown with **p**) is energetically more favorable than the path for OH attack on the terminal carbon (path containing structures shown with **p′**) atom since it has lower barriers and energetically rich intermediates that can easily overcome these barriers. It has been shown that in the conversion of hydroxyalkyl radicals to alkoxy radicals tunneling may be effective, which enables the reaction to proceed much more easily. [15, 22]

cis-2-Butene–OH reaction

cis-2-Butene (**c1**) has the most effective steric repulsion among the alkenes studied, and this causes the C1C2 bond to be the longest (1.347 Å).

The symmetry of *cis*-2-butene (**c1**) is conserved in the *cis*-2-butene–OH radical complex (**c2**). The C1H8 and C2H8 bond lengths are shorter as compared to the ones in the complex in propene (**p2**) due to the presence of the second methyl group, which increases the electron density significantly in the CC double bond of *cis*-2-butene.

The transition state **c3** has the longest CO bond of all (Fig. 3b). The OH group aligns itself on the opposite side of the methyl groups in order to minimize the steric repulsions between the oxygen lone pairs and the methyl group on C3.

The two structures for the hydroxybutyl radical **c4**, formed by the addition of the OH radical to *cis*-2-butene, are similar in geometry except for the orientation of the hydroxyl hydrogen (Fig. 4b). The C1C2 and C1C3 bonds differ slightly between these conformers due to the steric effects caused by the inward orientation of the hydroxyl hydrogen, and the conformer with the inward oriented hydrogen is more stable as in the case of the smaller alkenes.

The hydrogen transfer for the formation of butoxy radicals occurs via the transition state **c5**. The C1C2 and C1C3 bond lengths are the longest among all the transition states; however, the C2H8 bond is the shortest among all, indicating that the transition state **c5** is a relatively late transition state as compared to the others (Fig. 5b).

For the butoxy radical **c6**, two conformers having similar geometrical parameters are formed. The main difference between these conformers is the relative position of the C4 methyl group with respect to the oxygen. The methyl group on C4 is *gauche* to the oxygen atom in one of the conformers whereas it is *anti* to the same oxygen in the other conformer.

The *cis*-2-butene–OH complex (**c2**) is the most stable as compared to all the complexes and it is 4.67 kcal mol^{-1} more stable than the separated products (Table 3). The transition state **c3** is only 1.66 kcal mol^{-1} higher in energy than the complex **c2**. The largest energy difference between a transition state and a hydroxyalkyl radical is obtained between **c3** and **c4**. The hydroxybutyl radical **c4** is 31.00 kcal mol^{-1} lower in energy than the transition state **c3**. The transition state **c5** is only 1.08 kcal mol^{-1} higher than the initial reactants; this is the smallest value calculated for all the transition states in the alkene–OH reactions (Table 3). The barrier from **c4** to **c5** (35.09 kcal mol^{-1}) is comparable to the values obtained for OH addition to ethene or to the terminal carbon of propene but is higher than the values obtained for OH addition to the central carbon of propene or *trans*-2-butene. The butoxy radical **c6** has a relative energy of 29.05 kcal mol^{-1} as compared to the transition state **c5**.

trans-2-Butene–OH reaction

In contrast to *cis*-2-butene (**c1**), the methyl groups are located on opposite sides of the C1C2 bond minimizing the steric repulsion. As a result of this stabilization all the bond lengths and bond angles are smaller in *trans*-2-butene (**t1**) as compared to *cis*-2-butene (**c1**).

In the *trans*-2-butene–OH radical complex (**t2**), the C1H8 and C2H8 bonds are slightly longer than in the complex **c2** for *cis*-2-butene (Fig. 2a, b). When the OH radical approaches *trans*-2-butene (**t1**), there is always a methyl group that causes steric crowding, whereas for *cis*-2-butene (**c1**), one side is always sterically available for the OH radical attack. The symmetry is distorted by the differences between the C1H8O7 and C2H8O7 angles as well as the differences between the C3C1H8 and C4C2H8 angles.

The transition state **t3** has similar geometrical parameters to **c3** except for the orientation of the hydroxyl hydrogen H8 (Fig. 3b). The deviation from the plane of the C1C2 bond is less in **t3** as compared to the one in **c3** because of the environment as explained above.

As in the *cis*-2-butene–OH reaction, two hydroxybutyl radical conformers for the structure **t4** have been located for the *trans*-2-butene–OH reaction. There are two main differences between these conformers: the orientation of hydroxyl hydrogen and the position of methyl group with respect to the oxygen atom. Among the two, the one where the hydrogen is directed inwards and the methyl group *trans* to the oxygen is more stable. It is worth noting that in both compounds the methyl group is staggered to the oxygen atom.

The transition state for the hydrogen transfer (**t5**) has a shorter C1C2 bond and smaller C1C2C4 and C2C1C3

angles as compared to **c5** due to the change in the position of the methyl group on C2 (Fig. 5b). The other parameters are similar in **c5** and **t5**.

There is only one conformer (**t6**) for the butoxy radical formed in the *trans*-2-butene–OH reaction. In fact, two conformers have been optimized, but one of them is found to be the same with the least stable conformer optimized for *cis*-2-butene. The methyl groups are almost *anti* to each other with a deviation of 2.0° from the C3C1C2C4 plane. The methyl group on C2 is staggered to the oxygen atom.

trans-2-Butene (**t1**) is more stable than *cis*-2-butene (**c1**) by 1.52 kcal mol^{-1}. While comparing the energies of the compounds optimized in the reactions of *cis*- and *trans*-2-butene with the OH radical, this difference must be taken into account. The *trans*-2-butene–OH complex **t2** is 4.55 kcal mol^{-1} lower in energy as compared to the initial reactants. The barrier between the complex **t2** and the transition state **t3** (1.60 kcal mol^{-1}) is very close to the one obtained between **c2** and **c3** for *cis*-2-butene (1.66 kcal mol^{-1}). The hydroxybutyl radical **t4** has a relative energy of –33.25 kcal mol^{-1} and the following transition state **t5** is separated from **t4** by a barrier of 34.59 kcal mol^{-1} (Table 3). The transition state **t5** is only 1.34 kcal mol^{-1} higher in energy than the initial reactants; this value is the smallest except for the one for **c5** in the OH addition reaction to *cis*-2-butene. The most stable butoxy radical (**t6**) is formed in the reaction of *trans*-2-butene with a relative energy of –27.12 kcal mol^{-1} (Fig. 6b).

Conclusions

The formation of alkoxy radicals in the alkene–OH radical reactions has been thoroughly investigated in this work. The reactions of four simple alkenes (ethene, propene, *cis*- and *trans*-2-butene) have been modeled. The most interesting results have been obtained for the reaction of propene since it has two chemically nonequivalent atoms susceptible to OH attack. The calculations at the MP2 level have shown that the attack is most likely to occur on the central carbon atom of propene rather than the terminal carbon. This reaction path is preferable both kinetically and thermodynamically but the energy differences are quite dependent on the basis set used and on the inclusion of thermal corrections.

For all the alkene–OH reactions studied, the reaction starts with the formation of the alkene–OH complex since the transition states for the formation of hydroxyalkyl radicals are lower in energy than the initial reactants. The conversion of hydroxyalkyl radicals to alkoxy radicals by hydrogen transfer requires a relatively high barrier, which may be overcome by the excess energy formed in the formation of the hydroxyalkyl radical. As indicated in the literature, [15, 22] the tunneling effect may minimize the effect of the high barrier for that hydrogen transfer. The results have also confirmed that the conversion of hydroxyalkyl radicals to alkoxy radicals is endothermic.

Acknowledgements We are grateful to the Boğaziçi Üniversitesi Araştırma Fonu for the support provided to the project 98B504D. We would like to thank Prof. A. Vivier-Bunge for making her papers available for us prior to publication.

References

1. Bailey PS (1978, 1982) Ozonation in organic chemistry, vol 1, vol 2. Academic Press, New York
2. Atkinson R, Carter WPL (1984) Chem Rev 437–470
3. Atkinson R, Aschmann SM (1993) Environ Sci Technol 27: 1357–1363
4. Grosjean D, Grosjean E, Williams II EL (1994) Environ Sci Technol 28:1099–1105
5. Paulson SE, Orlando JJ (1996) Geophys Res Lett 23:3727–3730
6. Paulson SE, Chung MY Hasson AS (1999) J Phys Chem A 103:8125–8138
7. Neeb P, Moortgat GK (1999) J Phys Chem A 103:9003–9012
8. Martinez RI, Huie RE, Herron JT (1980) Chem Phys Lett 72:443–447
9. Tully FP (1983) Chem Phys Lett 96:148–153
10. Zellner R, Lorenz K (1984) J Phys Chem 88:984–989
11. Atkinson R (1987) Int J Chem Kinet 19:799–828
12. Wei-Guang Diau E, Lee YP (1992) J Chem Phys 96:377–386
13. Hatakeyama S, Lai H, Murano K (1995) Environ Sci Technol 29:833–835
14. Sosa C, Schlegel HB (1987) J Am Chem Soc 109:4193–4198
15. Sosa C, Schlegel HB (1987) J Am Chem Soc 109:7007–7015
16. Abbattt JPD, Anderson JG (1991) J Phys Chem 95:2382–2390
17. Villà J, González-Lafont A, Lluch JM, Corchado JC, Espinosa-García J (1997) J Chem Phys 107:7266–7274
18. Engels B, Peyerimhoff SD (1989) J Phys Chem 93:4462–4470
19. Engels B, Peyerimhoff SD, Sell PS (1990) J Phys Chem 94:1267–1275
20. Alvarez-Idaboy JR, Diaz-Acosta I, Vivier-Bunge A (1998) J Comput Chem 19:811–819
21. Sekusak S, Liedl KR, Sabljic A (1998) J Phys Chem A 102: 1583–1584
22. Yamada T, Bozzelli JW, Lay T (1999) J Phys Chem A 103: 7646–7655
23. Alvarez-Idaboy JR, Mora-Diez N, Vivier-Bunge A (2000) J Am Chem Soc 122:3715–3720
24. Møller C, Plesset MS (1934) Phys Rev 46:618–622
25. Pople JA, Binkley JS, Seeger R (1976) Int J Quantum Chem Symp 10:1–19
26. Frisch MJ, Head-Gordon M, Trucks GW, Foresman JB, Schlegel HB, Raghavachari K, Robb MA, Binkley JS, Gonzales C, Defrees DJ, Fox DJ, Whiteside RA, Seeger R, Melius CF, Baker J, Martin RL, Kahn LR, Stewart JJP, Topiol S, Pople JA (1994) Gaussian 94. Gaussian, Pittsburgh, Pa.
27. Singleton DL, Cvetanovic RJ (1976) J Am Chem Soc 98: 6812–6819
28. Mozurkewich M, Benson SW (1984) J Phys Chem 88:6429–6435
29. Bartels M, Hoyermann K, Sievert R (1982) Symp (Int) Combust 19:61–72
30. Cvetanovic RJ (1976) 12th International Symposium on Free Radicals, Laguna Beach, Calif.
31. Diaz-Acosta I, Alvarez-Idaboy JR, Vivier-Bunge A (1999) Int J Chem Kinet 31:29–36